Front. Phys. China, 2009, 4(3): 373–377
DOI 10.1007/s11467-009-0027-5

RESEARCH ARTICLE

Chiral selective tunneling induced graphene nanoribbon switch

Qin-wei SHI (石勤伟), **Zheng-fei WANG** (王征飞), **Qun-xiang LI** (李群祥), **Jin-long YANG** (杨金龙)(✉)

Hefei National Laboratory for Physical Sciences at the Microscale, University of Science and Technology of China, Hefei 230026, China
E-mail: jlyang@ustc.edu.cn

Received February 16, 2009; accepted February 19, 2009

An armchair graphene nanoribbon switch has been designed based on the principle of the Klein paradox. The resulting switch displays an excellent on–off ratio performance. An anomalous tunneling phenomenon, in which electrons do not pass through the graphene nanoribbon junction even when the conventional resonance condition is satisfied, is observed in our numerical simulations. A selective tunneling rule is proposed to explain this interesting transport behavior based on our analytical results. Based on this selective rule, our switch design can also achieve the confinement of an electron to form a quantum qubit.

Keywords switch, Klein paradox, graphene nanoribbon, selective tunneling

PACS numbers 85.65.+h, 73.63.-b, 73.61.Wp

1 Introduction

The recent fabrication of graphene has attracted a lot of research interest [1–6]. Graphene consists of a single atomic layer of graphite arranged in a honeycomb pattern, which has been shown to be a remarkable conductor in which electrons behave as massless, relativistic particles [1–3]. Recently, Geim's group proposed an experimental realization predicting the so-called Klein paradox in a two-dimensional (2-D) graphene system [7]. The Klein paradox is a counterintuitive relativistic process in which the electron can pass through a potential barrier without exponential decay if its height exceeds the electron's rest energy [7, 8]. Based on this Klein paradox design, graphene-based field effect transistors (FET) could be achieved, but these transistors have poor on–off ratios due to the minimal conductivity of the 2-D graphene structure [1, 7].

A simple type of graphene based quasi-one-dimensional system with nanometer sized width, referred to as graphene nanoribbons, has been studied extensively [9, 10, 13–19]. The edge carbon atoms of graphene nanoribbons have two typical topological shapes: namely armchair and zigzag. Zigzag graphene nanoribbons (ZGNRs) have a localized state near the Fermi level, which originates from a gauge field produced by lattice deformation [9]. Such a localized state, however, does not appear in armchair graphene nanoribbons (AGNRs). The energy gap of AGNRs can be easily tuned by controlling its width [10]. This remarkable characteristic is very attractive in making graphene nanoribbon based nanoscale devices. Moreover, a graphene nanoribbon is easier to manipulate than a carbon nanotube (CNT, which can be used to produce switch and rectifier [11, 12]) due to its flat structure, and thus it can be tailored by using conventional lithography techniques.

Here, we design a graphene nanoribbon switch by utilizing the principle of the Klein paradox and study the associated tunneling problem in a quasi-one-dimensional system. We show that our designed switch overcomes the intrinsic limit of the 2-D graphene switch, and displays an excellent on–off ratio performance.

2 Model and computational method

We consider a semiconducting AGNR connecting to left and a right metallic armchair graphene leads. Due to the band gap in our junction, the electron within the energy gap is prohibited to transmit through the junction without an applied gate voltage, and the graphene switch stays in the "off" state. The junction can be turned "on" when an external gate voltage exceeds a thresh-

old voltage. The applied gate voltage shifts the valence subbands of the graphene nanoribbon upwards to serve as conducting channels. This observation realizes the main feature described by Klein paradox and the electron can pass through the high potential barrier. Our setup is shown in Fig. 1. The bottom subgraph of Fig. 1 shows the atomic structure of the graphene junction including three regions: left lead, middle graphene region, and right lead. Both leads have the same width with $W = 3m - 1$ to ensure that they are metallic within tight-binding approximation (actually, the AGNRs with such a width are semiconductor with the least energy gap at the density functional theory level [12]). The width of the middle region is chosen to be $W+4$ so that it is semiconducting [10]. The top subgraph in Fig. 1 shows the dispersion relation of the left, middle and the right region of the switch, respectively. The dashed line denotes the energy E of incident electrons. U is the external potential applied to the middle graphene region. Unlike the conventional parabolic semiconductor energy band diagram ($\boldsymbol{E} \propto \boldsymbol{k}^2$), the energy of the lowest conduction subband in the lead is linearly proportional to the vector $\boldsymbol{k}$ [2]. This dispersion relation indicates that carriers in this channel are massless.

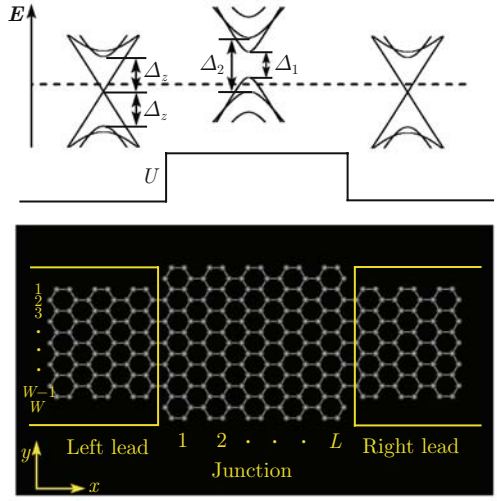

Fig. 1 Schematic diagrams of the energy band dispersions and the proposed graphene switch.

The conductance G of the switch is calculated by using the Landauer-Büttiker formula $\left(G=\frac{2e^2}{h}T\right)$[20]. The transmission function T is obtained by the recursive Green's function method [21, 22]. Here, we assume that edge bonds of the graphene nanoribbon are saturated by hydrogen atoms, no defects and distortion exist in system. In order to ensure the incident electron energy lies within the single-mode region of the leads and also in the gap of the middle graphene region, we choose $E<\min\left(\frac{\Delta_1}{2}, \Delta_z\right)$. As shown in Fig. 1, Δ_1 is the band gap between the lowest conduction subband and the upmost valence subband of the junction, Δ_z is the energy spacing between the bottom of conduction subbands and the next subband within the lead. In the following simulations, we set W=23 and thus obtain the corresponding Δ_z=0.65 eV, Δ_1=0.38 eV and Δ_2=0.79 eV by the nearest neighbor tight-binding band structure calculation [22].

3 Results and discussion

The calculated conductances are shown in Fig. 2. By applying an external gate voltage at the middle graphene region, a potential barrier U appears. In general, if the chosen voltage potential makes the energy of incident electron touch the first top of the valence subband of the junction, the incident electron can easily pass through the junction as expected and the switch should be turned "on". However, our simulation result shows that the incident electrons are almost reflected completely and the conductance remains almost zero. This phenomenon implies that the carrier has to satisfy an additional condition to pass through the potential barrier.

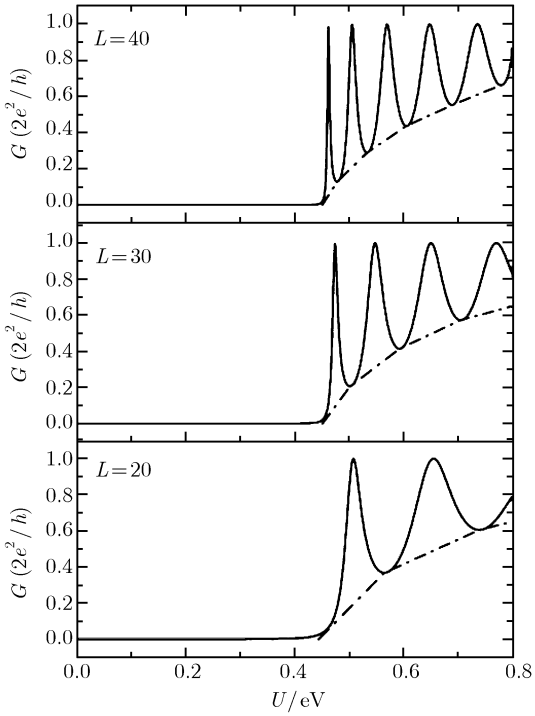

Fig. 2 Conductance vs. the potential height in the single-mode region with different length of the junction. Here W = 23 and E = 0.05 eV. The conductance oscillates above the envelope line plotted with dash dot line.

When the potential barrier U increases further, the switch turns "on" and the first resonant transmission peak appears around U=0.51 eV for L=20. This behavior can be easily understood by the Klein's paradox. That is, with the help of the hole's channels, the electrons can transfer through the large potential barrier without exponential decay. The conductance oscillates

above the envelope line and increases as U increases due to the resonance and antiresonance transports, as shown in Fig. 2. Although more channels can allow electrons to pass through and more resonance matching conditions can be satisfied as U increases, T never exceeds 1. The reason is that the energy of the incident electron is limited within the single-mode region in our calculations. As the length of the junction increases, the first resonant peak becomes sharper and shifts towards the left slightly and more resonant peaks appear. These observations can be easily understood by the conventional resonance condition. However, to produce the first conductance peak, the condition $U > \Delta_2/2 + E$=0.44 eV is still required. This result strongly suggests that this peak results from the second valence subband.

To verify the above conjecture, Fig. 3 shows the conductance as a function of the junction length L calculated by fixing E=0.05 eV and U=0.5 eV. Such a choice provides two conducting channels in the middle region for electrons passing through the junction. In general, the conductance curve should be complicated with some glitches due to the quantum interference between two channels [23]. Surprisingly, our numerical result exhibits a regular periodicity as a function of L in Fig. 3. Based on the detailed analysis of this conductance period with the conventional resonance condition, we find that only the second valence subband provides a channel to allow incident electrons to pass, and the first valence subband does not contribute. We also perform similar simulations with different widths (W=17 and 20) and the same phenomenon is observed.

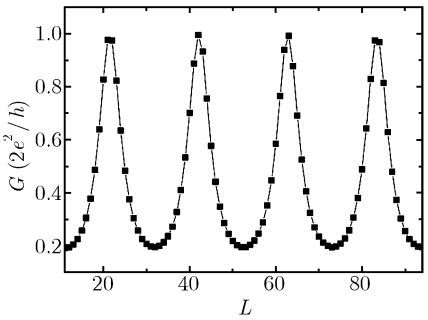

Fig. 3 Conductance versus the length of the junction with W = 23, E = 0.05 eV and U = 0.5 eV.

Generally speaking, to pass through the middle region, electrons have to satisfy the conventional resonance condition which usually describes the transfer of an electron through a junction via resonant tunneling (T = 1) due to the phase accumulation. It works well in conventional semiconductors when the Schrödinger equation is used. In our switch model, the valence subbands in the middle region can be shifted upwards with the applied external gate voltage to provide conducting channels. When electrons satisfy the conventional resonance condition, $q_x L = N\pi$ with N=0, ±1, ±2, ⋯. Here, q_x denotes the x-direction (along the propagation direction) component of the wave-vector inside the middle region; they can pass through the junction resonantly. However, our simulation results show that the electron is still prohibited to pass through the middle region when the conventional resonance condition is satisfied. To understand this anomalous transport behavior more clearly, we derive an analytical expression of the eigenfunction and eigenvalue of the perfect armchair graphene nanoribbon with a finite width (W) as [24]:

$$\psi_n^s(j,q_x) = \frac{\sin\left(q_n\frac{\sqrt{3}}{2}aj\right)}{\sqrt{(W+1)\frac{\sqrt{3}}{2}a}}\begin{pmatrix}1\\ s\sqrt{\frac{\mu^*}{\mu}}\end{pmatrix} \tag{1}$$

$$\varepsilon_n^s(q_x) = sV\sqrt{\mu\mu^*} \tag{2}$$

with $\mu = 2e^{iq_x\frac{a}{2}}\cos\left(q_n\frac{\sqrt{3}}{2}a\right) + e^{-iq_x a}$, $q_n = n\pi/\left[\frac{\sqrt{3}}{2}a \cdot (W+1)\right]$, respectively. Here, a is the C–C bond length (1.42 Å), V is the nearest hopping parameter (−3.0 eV), n denotes different subband with 1, ⋯, W, j labels the atomic position in the y-direction with 1,⋯, W, and s=+1 (−1) describes the conduction (valence) subbands, respectively. The chirality of the electron in the conduction subband or hole in the valence subband can be determined by the good quantum number q_x and q_n. To determine the lowest conduction subband or the upmost valence subband, the integer number n needs to satisfy the condition $n = Nint\left[\frac{2}{3}(W+1)\right]$. Here the function of *Nint* rounds off the variable to an integer. To verify that electrons in the lowest conduction subband cannot pass through the switch via the upmost valence subband of the middle region, we calculate the corresponding transfer matrix element P_{11}, and we obtain $P_{11} = |\langle s,n,q_x|\hat{V}|s',n',q_x'\rangle|^2 \approx 4.5\times10^{-14}$ eV^2 with W=23, s=+1, n=16, s'=−1, and n'=19. Here, $\hat{V} = V\sum_j |j\rangle\langle j+2|$ with j=2, 4, 6, ⋯, $W-1$ is the scattering operator coming from the sharp interface between the lead and the middle region. In the elastic scattering process in our system, the equation $\varepsilon_n^{+1}(q_x) = \varepsilon_{n'}^{-1}(q_x') + U$ has to be satisfied. Meanwhile, the applied voltage U is large enough to ensure the equation has a real numerical solution (q_x'). The transfer matrix element P_{12} between the lowest conduction subband to the second upmost valence subband is calculated to be around 0.27 eV^2. In our switch the value of these transfer matrix elements are almost independent of the width of graphene nanoribbon based on our numerical simulations.

The sharp interface in our design plays an important role, which was not observed in its 2-D counterpart [7]. From our numerical results, it is clear that the selective

tunneling corresponding to two transfer matrix elements (P_{11} and P_{12}) can illustrate the interesting transport process. When U>0.24 eV, the first valence subband of the middle region is moved high enough to provide a conducting channel, but P_{11} almost equals to zero. That is to say, no matter whether the chirality of electrons conserves or not, the sharp interface in this symmetrical connection prevents the tunneling process. Electrons, therefore, are bounced back and the conductance remains almost zero, as shown in Fig. 2. Increasing the length of the junction only changes the conventional resonance condition, but the conductance still remains zero. When we further increase the voltage potential to U>0.44 eV, the second valence subband of the middle region moves upwards. The energy of incident electrons touches this channel and the electrons can then tunnel through the potential barrier without exponential decay. Considering the symmetry of the band structure of the junction, the selective tunneling behavior can also be observe when applying a negative gate voltage in the junction region.

Note that whether the first valence subband contributes to the conductance or not depends strongly on the geometric structure of the graphene nanoribbon junction. As an example, a T-shaped junction with the same width of the previous symmetry structure is shown in Fig. 4. By choosing the same parameters (E=0.05 eV, W=23 and L=20) as in the case of Fig. 3, numerical results in Fig. 4 show clearly that the first conductance peak appears in the region where the incident energy touches the first valence subband (0.24 eV<U<0.44 eV). The reason is that the transfer matrix element (P_{11}) has a finite value (about 0.24 eV^2) in the T-shaped junction. Our results suggest that the switch conducting behavior can be manipulated by tailoring the graphene nanoribbon. In the range of 0.44 eV<U<

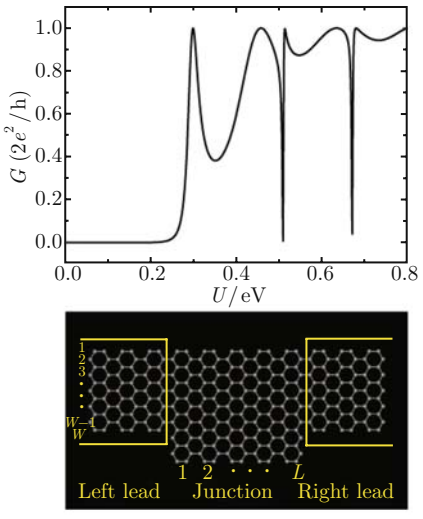

Fig. 4 Top subgraph: conductance vs. the potential height in the single-mode region. Bottom subgraph: atomic structure of the T-shaped junction. Here W = 23, L = 20 and E = 0.05 eV.

0.7 eV, another interesting observation is that two obvious conductance dips appear in the conductance curve. This phenomenon can be attributed to the destructive interference effect between two conducting channels [25]. Recently, Li *et al.* [26] have predicted that the transport properties of ZGNRs also depend on the symmetry with respect to the midplane between two edges. Asymmetric ZGNRs behave as conventional conductors, while symmetric ZGNRs exhibit very small currents. This difference comes from different coupling between the frontier subbands, which is dependent on the symmetry of the systems [26].

To illustrate the switch effect more clearly in the single-mode region, Fig. 5 presents a three-dimensional color picture to display the conductance as a function of incident electron energy (E) and the potential barrier height (U) for the configuration shown in Figure 1. The color is scaled with the corresponding conductance, white and blue colors correspond to T = 1 ("on") and T = 0 ("off"), respectively. It is clear that the figure can be roughly divided into two regions bounded by the first peak (*the leftmost white line*). At the left of the first peak (*the first white line*), the switch stays shut off or all incident electrons are bounced back. The junction begins to be turned "on" starting from the right of the first peak by applying a certain threshold bias U and its conductance oscillates with increasing U as shown in Fig. 2. Although more channels can allow electrons to pass through or more resonance matching conditions can be satisfied as U increases, T never exceeds 1. The reason is that the energy of incident electron is limited within the single-mode region in our calculations. Several additional interesting features can be observed in Fig. 5: (i) the peaks or the white lines are parallel to each other and shift toward the right as the incident energy increases. (ii) all peaks are straight lines indicating the required voltage to open the switch increases linearly as incident electron energy increases. (iii) the white lines become wider and blue lines become narrower as U increases.

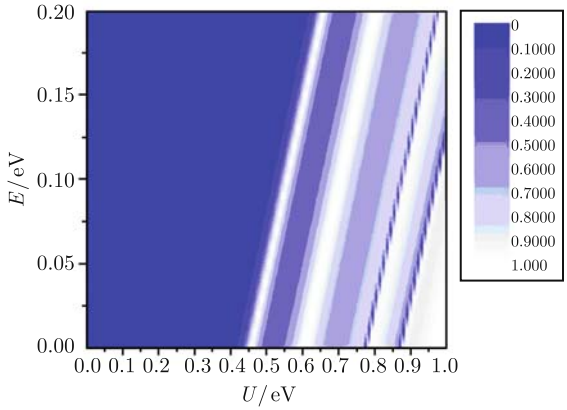

Fig. 5 Three-dimensional plot of conductance as the function of energy and potential height for the configuration shown in Fig. 1. Here W=23 and L=20.

The confinement of electrons is a basic requirement to realize a qubit in a solid device. In addition to the switch design, the selective tunneling rule observed in the symmetrical nanoribbon suggests that we can achieve the confinement of an electron in the middle region even though the region connects to two metallic leads. The condition for such a confinement is $\Delta_z > |\Delta_1 + U|$. The external bias voltage U can be adjusted to control whether the trapped electrons pass through the middle region or not. Our design is easier to implement than that in Ref. [24]. Compared to that in a GaAs quantum dot, our qubit design in graphene nanoribbon is very promising because the spin–orbit interaction and hyperfine interaction in graphene are considerably weak [21]. Spin coherence length is expected to be $L \sim 10$ μm in a disordered graphene [27]. We can exploit the electron–spin freedom to design quantum qubit using our proposed device. As a result, the qubit in the graphene nanoribbon can possibly be operated at room temperature.

4 Summary

In conclusion, the transport properties of a semiconducting graphene nanoribbon sandwiched between two metallic graphene nanoribbon leads are investigated. Switching behavior is observed according to our numerical results. The junction has a good on–off ratio performance, which is almost completely pinched-off without external gate voltage and can be turned "on" by applying a threshold bias voltage. We find that our numerical results are related closely to the Klein phenomenon. Electrons can pass through the junction when these Dirac Fermions satisfy both the conventional resonance condition and the selective tunneling rule. These findings are helpful for us to construct and design graphene nanoelectronic devices in the near future. For instance, the proposed graphene switch can be used to achieve qubit design in quantum computers [28].

Acknowledgements This work was partially supported by the National Natural Science Foundation of China, the National Key Basic Research Program, the Science and Technological Fund of Anhui Province for Outstanding Youth, the USTC-HP HPC project, and the SCCAS and Shanghai Supercomputer Center.

References

1. K. S. Novoselov, A. K.Geim, S. V. Morozov, D. Jiang, Y. Zhang, S. V. Dubonos, I. V. Grigorieva, and A. A. Firsov, Science, 2004, 306: 666
2. K. S. Novoselov, A. K. Geim, S. V. Morozov, D. Jiang, M. I. Katsnelson, I. V. Grigorieva, S. V. Dubonos, and A. A. Firsov, Nature (London), 2005, 438: 197
3. Y. B. Zhang, Y. W. Tan, H. L. Stormer, and P. Kim, Nature (London), 2005, 438: 201
4. C. Berger, Z. M. Song, X. B. Li, X. S. Wu, N. Brown, C. Naud, D. Mayou, T. B. Li, J. Hass, A. N. Marchenkov, A. H. Conrad, P. N. First, and W. A. de Heer, Science, 2006, 312: 1191
5. T. Ohta, A. Bostwick, T. Seyller, K. Horn, and E. Rotenberg, Science, 2006, 313: 951
6. S. Stankovich, D. A. Dikin, G. H. B. Dommett, K. M. Kohlhaas, E. J. Zimney, E. A. Stach, R. D. Piner, S. T. Nguyen, and R. S. Ruoff, Nature (London), 2006, 442: 282
7. M. I. Katsnelson, K. S. Novoselov, and A. K. Geim, Nature Phys., 2006, 2: 620
8. O. Klein, Z. Phys., 1927, 53: 157
9. K. Sasaki, S. Murakami, and R. Saito, J. Phys. Soc. Jpn., 2006, 75: 074713
10. K. Nakada, M. Fujita, G. Dresselhaus, and M. S. Dresselhaus, Phys. Rev. B, 1996, 54: 17954
11. M. R. Diehl, D. W. Steuerman, H. Tseng, S. A. Vignon, A. Star, P. C. Celestre, J. F. Stoddart, and J. R. Heath, Chem PhysChem, 2003, 4: 1335
12. A. N. Andriotis, M. Menon, D. Srivastava, and L. Chernozatonskii, Phys. Rev. Lett., 2001, 87: 066802
13. V. Barone, O. Hod, and G. Scuseria, Nano Lett., 2006, 6: 2748
14. Y. W. Son, M. L. Cohen, and S. G. Louie, Nature (London), 2006, 444: 347
15. Y. W. Son, M. L. Cohen, and S. G. Louie, Phys. Rev. Lett., 2006, 97: 216803
16. M. Fujita, K. Wakabayashi, K. Nakada, and K. Kusakabe, J. Phys. Soc. Jpn., 1996, 65: 1920
17. K. Wakabayashi, Phys. Rev. B, 2001, 64: 125428
18. J. Tworzydlo, B. Trauzettel, M. Titov, A. Rycerz, and C. W. J. Beenakker, Phys. Rev. Lett., 2006, 96: 246802
19. Z. F. Wang, Q. X. Li, H. X. Zheng, H. Ren, H. B. Su, Q. W. Shi, and J. Chen, Phys. Rev. B, 2007, 75: 113406
20. R. Landauer, Philos. Mag., 1970, 21: 863
21. J. Zhang, Q. W. Shi, and J. L. Yang, J. Chem. Phys., 2004, 120: 7733
22. S. Datta, Electronic Transport in Mesoscopic Systems, New York: Cambridge University Press, 1995
23. C. P. Chang, Y. C. Huang, C. L. Lu, J. H. Ho, T. S. Li, and M. F. Lin, Carbon, 2006, 44: 508
24. H. X. Zheng, Z. F. Wang, T. Luo, Q. W. Shi, and J. Chen, Phys. Rev. B, 2007, 75: 165414
25. K. Wakabayashi and M. Sigrist, Phys. Rev. Lett., 2000, 84: 3390
26. Z. Y. Li, H. Y. Qian, J. Wu, B. L. Gu, and W. H. Duan, Phys. Rev. Lett., 2008, 100: 206802
27. D. Huertas-Hernando, F. Guinea, and A. Brataas, Eur. Phys. J. Special Topics, 2007, 148: 177
28. B. Trauzette, D. V. Bulaev, D. Loss, and G. Burkard, Nature Phys., 2007, 3: 192